Dental Materials Journal 2013; 32(2): 274–280

Influence of surface treatment of yttria-stabilized tetragonal zirconia polycrystal with hot isostatic pressing on cyclic fatigue strength

Toshihiko IIJIMA[1,2], Shinya HOMMA[1,2], Hideshi SEKINE[1,3], Hodaka SASAKI[1,2], Yasutomo YAJIMA[1,2] and Masao YOSHINARI[1]

[1] Division of Oral Implants Research, Oral Health Science Center, Tokyo Dental College, 1-2-2, Masago, Mihama-ku, Chiba 261-8502, Japan
[2] Department of Oral and Maxillofacial Implantology, Tokyo Dental College, 1-2-2 Masago, Mihama-ku, Chiba 261-8502, Japan
[3] Division of Oral Implant Service, Department of Clinical Oral Health Science, Tokyo Dental College, 2-9-18 Misakicho, Chiyoda-ku, Tokyo 101-0061, Japan
Corresponding author, Masao YOSHINARI; E-mail: yosinari@tdc.ac.jp

Hot isostatic pressing processed yttria-stabilized tetragonal zirconia polycrystal (HIP Y-TZP) has the potential for application to implants due to its high mechanical performance. The aim of this study was to investigate the influence of surface treatment of HIP Y-TZP on cyclic fatigue strength. HIP Y-TZP specimens were subjected to different surface treatments. Biaxial flexural strength was determined by both static and cyclic fatigue testing. In the cyclic fatigue test, the load was applied at a frequency of 10 Hz for 10^6 cycles in distilled water at 37°C. The surface morphology, roughness, and crystal phase of the surfaces were also evaluated. The cyclic fatigue strength (888 MPa) of HIP Y-TZP with sandblasting and acid-etching was more than twice that of Y-TZP as specified in ISO 13356 for surgical implants (320 MPa), indicating the clinical potential of this material.

Keywords: Zirconia, Y-TZP, Surface topography, Hot isostatic pressing, Fatigue strength

INTRODUCTION

Zirconia, and yttria-stabilized zirconia (Y-TZP) in particular, are often used for the framework of fixed prostheses and dental implants when a metal-free restoration is required due to their mechanical, biocompatible and esthetic performance[1-3], and may overcome the drawback of titanium (Ti) implants that have gray coloring and risk of its hypersensitivity[4,5].

Zirconia implants have shown direct bone apposition and high stability *in vivo*[6]. Other studies reported that no fibrous tissues were detected at the implant-bone interface on loaded or unloaded zirconia implants[7], and newly formed bone was observed on zirconia surfaces in a rabbit study, together with close bone-to-implant contact of 68.4%[8]. These reports indicate that zirconia ceramics are suitable for use in dental implants. Recent research has focused on increasing bone-to-implant contact and speed of bone formation. Sennerby *et al.* reported a strong bone tissue response after 6 weeks of healing in rabbit bone on zirconia with two different topographies by surface modification[9]. Surface treatment of zirconia implants yielded an up to four-to-five-fold increase in resistance to torque compared with machining, suggesting that surface treatment increases bone stability[9].

One negative physical characteristic of Y-TZP, however, was reported to be low-temperature degradation[10,11] initiated in isolated surface grains, between which water is incorporated into the zirconia lattice through dissolution of Zr-O-Zr bonds and filling of oxygen vacancies[12]. This may result in a significant reduction in the strength and toughness of Y-TZP[13], a problem that is further exacerbated by exposure of the restoration to cyclic stresses such as chewing[14]. Thus, conventional half-sintering of a Y-TZP compact followed by air sintering at around 1,350°C does not produce a material of sufficient strength for clinical application, indicating the need for a method of increasing the strength of this material.

Hot isostatic press (HIP) processing under high pressure in an argon gas atmosphere is considered suitable for the implant body, as dental implants are not fabricated for the individual patient. Therefore, high mechanical performance can be ensured by HIP processing without resort to a complicated fabricating procedure. This method of processing affords very high density, enhancing the reliability of the ceramic components[15,16].

Given that the ceramic implant will be subjected to a humid environment and mastication in the oral cavity, cyclic fatigue tests are essential in assuring their success. Some recent studies have used cyclic loading to determine the durability of such implants under clinical conditions[17] rather than the static loading conventionally used[18,19].

Grinding, sandblasting, or acid-etching should be used to enhance osseointegration when zirconia is used for the implant body. However, this may induce phase transformation in zirconia, from tetragonal to monoclinic, as well as superficial microcracks, resulting in change in its mechanical properties in terms of both static and fatigue strength[20-22]. Takano *et al.* reported that the static and cyclic fatigue strength of Y-TZP with surface treatment was approximately 800 MPa and 394 MPa, respectively. Meanwhile, the static and cyclic fatigue strength of NANOZR with surface treatment was approximately 1,111 MPa and 667 MPa[23], respectively.

Received Sep 19, 2012: Accepted Dec 25, 2012
doi:10.4012/dmj.2012-247 JOI JST.JSTAGE/dmj/2012-247

However, the influence of surface treatment on the fatigue strength of Y-TZP fabricated by HIP processing (HIP Y-TZP) remains to be determined, even though this is an important factor in its durability in the oral environment[8,24,25].

Therefore, the aim of this study was to evaluate the influence of surface treatment of HIP Y-TZP on cyclic fatigue strength.

MATERIAL AND METHOD

Disk specimen preparation

Yttria-stabilized zirconia polycrystal powders (ZrO_2: balanced, Y_2O_3: 5.16 mass%, Al_2O_3: 0.25 mass%, Na_2O: 0.021 mass%, SiO_2: 0.007 mass%, Fe_2O_3: 0.003 mass%) (TZ-3YB-E; Tosoh, Tokyo, Japan) were processed by cold isostatic pressing into cylindrical rods. After peeling off the surface of the rods, they were sintered at 1,350°C for 2 h under air atmosphere (Y-TZP). Subsequently, HIP processing of the rods was performed at 1,300°C for 1 h under 147 MPa pressure in an argon atmosphere to produce HIP Y-TZP.

Disk specimens (13 mm in diameter, 0.5 mm in thickness) were prepared by cutting the rods with a diamond wheel. These HIP Y-TZP disks were randomly divided into 4 groups for preparation on both sides of each disk as shown in Table 1: (1) mirror-polished (MS); (2) sandblasted with 50-µm alumina (SB50); (3) sandblasted with 150-µm alumina (SB150); and (4) sandblasted with 150-µm alumina and acid-etched (SB150E). A polishing machine was used for the MS group (Ecomet 3, Buehler, Lake Bluff, IL, USA), which first ground the disks with diamond (70-µm and 45-µm) and then polished them with a polishing cloth incorporating 9-µm and 3-µm diamond and 0.6-µm colloidal silica to create mirror-polished surfaces. The sandblasted specimens were perpendicularly sandblasted from a distance of 10 mm with 50-µm or 150-µm alumina particles at 0.4 MPa air pressure. The SB150E specimens were prepared by etching SB150 with 47% hydrofluoric acid (HF) at room temperature for 15 min. These specimens were cleaned ultrasonically using acetone and distilled water for 10 min.

Microscopic observation and surface roughness

Microscopic observation was conducted to characterize the surface microstructure of each group using a scanning electron microscope (SEM) (SU6600, Hitachi, Tokyo, Japan). Fractured surfaces were also observed after the cyclic fatigue test.

The surface roughness of the specimens was analyzed using a surface roughness tester (Surfcom130A, Accretech, Tokyo, Japan). Four measurements were performed for each specimen according to ISO4287. The arithmetical mean deviation of the assessed profile (Ra) was measured under these conditions: cut-off value of 0.8 mm, measurement length of 4.0 mm, and measurement speed of 0.6 mm/s.

Table 1 Surface treatment

Code	Treatment
MS	Mirror-polished finally with colloidal silica
SB50	Sandblasted with 50 µm-alumina
SB150	Sandblasted with 150 µm-alumina
SB150E	Etched SB150 with HF(47%) for 15 min

Biaxial flexural strength in static test (static strength)

Five specimens from each group were used to measure biaxial flexural strength in the static test using a universal testing machine (AG-I 20 kN, Shimadzu, Kyoto, Japan) with a cross-head speed of 0.5 mm/min in air at room temperature. Disk specimens were placed on 3 steel spheres positioned 120 degrees apart in a circle (8.0 mm in diameter). A flat-end loading cylinder with a radius of 0.8 mm was then applied. Biaxial flexural strength was calculated using the equation listed in ISO 6872, with a Poisson's ratio value of 0.25 for each specimen.

Biaxial flexural strength in cyclic fatigue test (cyclic fatigue strength)

A servo-hydraulic universal testing machine (EHF-F05, Shimadzu) was used to determine cyclic fatigue strength by applying a cyclic load in the biaxial flexure mode at a frequency of 10 Hz for 10^6 cycles in distilled water at 37°C.

Cyclic fatigue strength was determined in each group by the staircase method, in which stress is raised in increments of 5%. First, 70%–80% of maximum load was applied to the specimen. If that specimen then fractured in less than 10^6 cycles of loading, a stress level one increment lower was applied to the next specimen. If this next specimen did not fracture at 10^6 cycles of loading, a load one increment higher was applied to the next specimen. This procedure was continued until the 20 specimens in each group were expended. The mean and standard deviation of fatigue strength were determined by the staircase method[26]. The calculation of the mean and standard deviation of the cyclic fatigue force is determined by the following equations.

$$m=y'+d(A/N),\quad s=d\sqrt{\frac{NB-A^2}{(N-1)N}}$$

where, m=statistical estimate of mean cyclic fatigue force, y'=lowest load level at which the less frequent event occurred, d=step size, *i.e.* the load increment, N=total number of less frequent events (Σn_i), s=statistical estimation of standard deviation. The lowest stress level considered was designated as i=0, the next stage as i=1, and so on until n_i, which was the number of failures or non-failures at a given stress level. $A=\Sigma i n_i$, $B=\Sigma i^2 n_i$.

The circle sign (○) is used if the less frequent event

is non-fracture and the cross sign (×) is used if the less frequent event is fracture.

X-ray diffractometry

The amount of monoclinic and tetragonal phase at before and after fatigue testing was determined in each specimen using an X-ray diffraction system (XRD) (RINT-2000, Rigaku, Tokyo, Japan) equipped with a position-sensitive proportional counter. The X-ray output was set at Cu-Kα, 40 kV and 200 mA. For measurement, the incident beam was focused onto a beam spot 100 μm in diameter using a collimator. X-ray diffraction measurement was performed around the center of the tensile stress side of each specimen, the point of cyclic loading, at before and after fatigue testing. Three specimens were used for each condition, each of which was measured at 3 points. The relative amount of monoclinic phase was calculated based on the method of Garvie and Nicholson[27].

Statistical analysis

Surface roughness value (Ra), biaxial strength, and monoclinic crystal content were statistically analyzed with an ANOVA followed by the Bonferroni test (α=0.01).

RESULTS

Microscopic observation and surface roughness

Representative SEM images of specimens from each group are shown in Fig. 1. The surface of MS was completely smooth, whereas that of SB50 and SB150 showed a rough texture. A large-waved configuration with comparatively deep defects were observed in SB150E including HIP Y-TZP nano-particles originated in the pre-sintered raw material. Little irregularity was observed in SB50 or SB150, however.

The Ra value depended on the size of alumina particle used for blasting (SB50, SB150), as summarized in Fig. 2. The Ra value increased in the order of SB50, SB150, and SB150E (p<0.01).

Biaxial flexural strength in static test (static strength)

Figure 3 shows the average and standard deviations of biaxial flexural strength in the static test. Biaxial flexural strength decreased in the order of SB150, SB150E (p<0.01).

Biaxial flexural strength in cyclic fatigue test (cyclic fatigue strength)

Cyclic fatigue strength at 10^6 cycles as determined by the staircase method is shown in Figs. 4a–d. Mean cyclic fatigue strength and standard deviation with each type of surface treatment at 10^6 cycles are shown in Fig. 5.

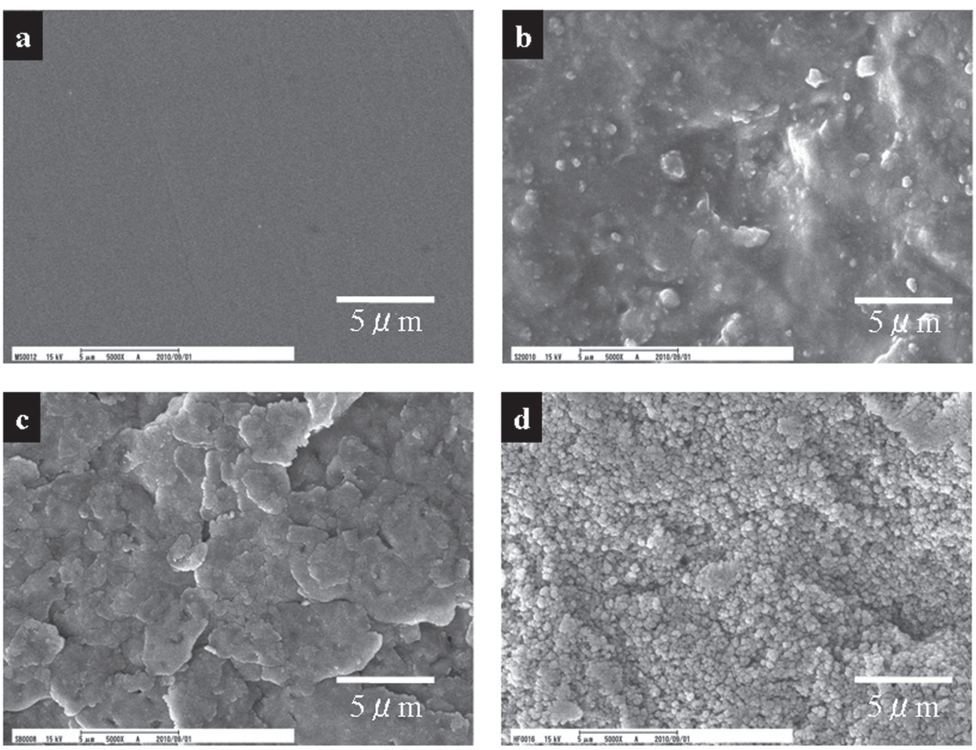

Fig. 1 SEM images of HIP Y-TZP surface.
(a) MS ×5,000; (b) SB50 ×5,000; (c) SB150 ×5,000; (d) SB150E ×5,000

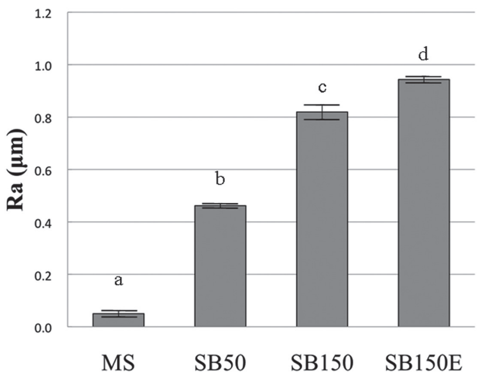

Fig. 2 Surface roughnes value (Ra μm) of MS, SB50, SB150 and SB150E.
Identical letter indicates no significant difference (p>0.01).

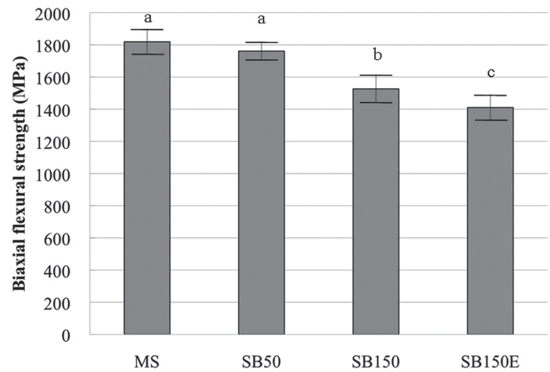

Fig. 3 Biaxial flexural strength of HIP Y-TZP disks with each type of surface treatment (static test).
Identical letter indicates no significant difference (p>0.01).

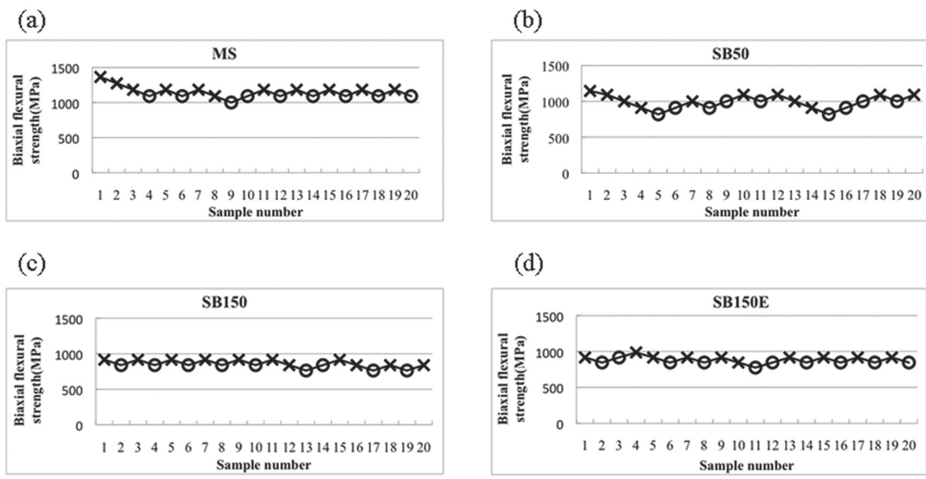

Fig. 4 Results of staircase method to determine mean fatigue strength at 10^6 cycles.
(a) MS, (b) SB50, (c) SB150, (d) SB150E ×: Fracture ○: Non-fracture

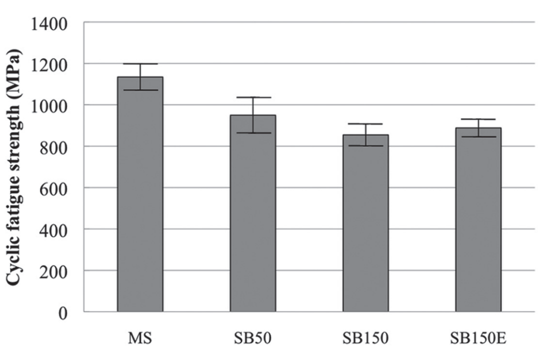

Fig. 5 Mean cyclic fatigue strength in MS, SB50, SB150 and SB150E.

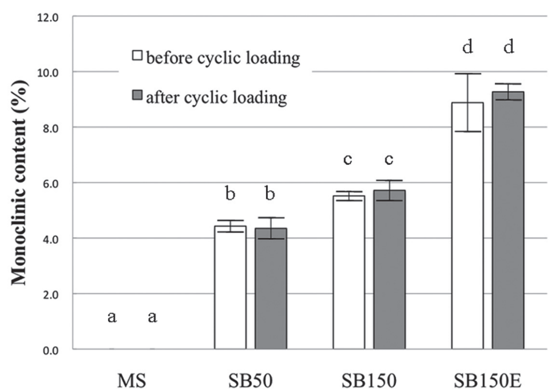

Fig. 6 Monoclinic content of HIP Y-TZP at before and after fatigue in each group.
No significant difference was observed in monoclinic content between before and after cyclic fatigue test.
Identical letter indicates no significant difference (p>0.01).

The cyclic fatigue strength of MS, SB50, SB150, and SB150E was 62.4%, 53.9%, 56.0%, and 63.0% of static strength, respectively. Cyclic fatigue strength ranged between 888.3 and 1,134.5 MPa depending on type of surface treatment.

X-ray diffractometry

Amount of monoclinic phase at before and after fatigue testing in each group is shown in Fig. 6. The monoclinic phase increased in SB50, SB150, and SB150E compared with in MS at both before and after the cyclic fatigue test ($p<0.01$). No significant difference was observed in monoclinic content between before and after the cyclic fatigue test.

Fractured surfaces

Figure 7 shows the tensile stress side surface of a fractured specimen after the cyclic fatigue test at magnifications of ×50, ×1,000, and ×3,000. Microcracks (white arrow) were observed originating in fractures close to the center of the specimen.

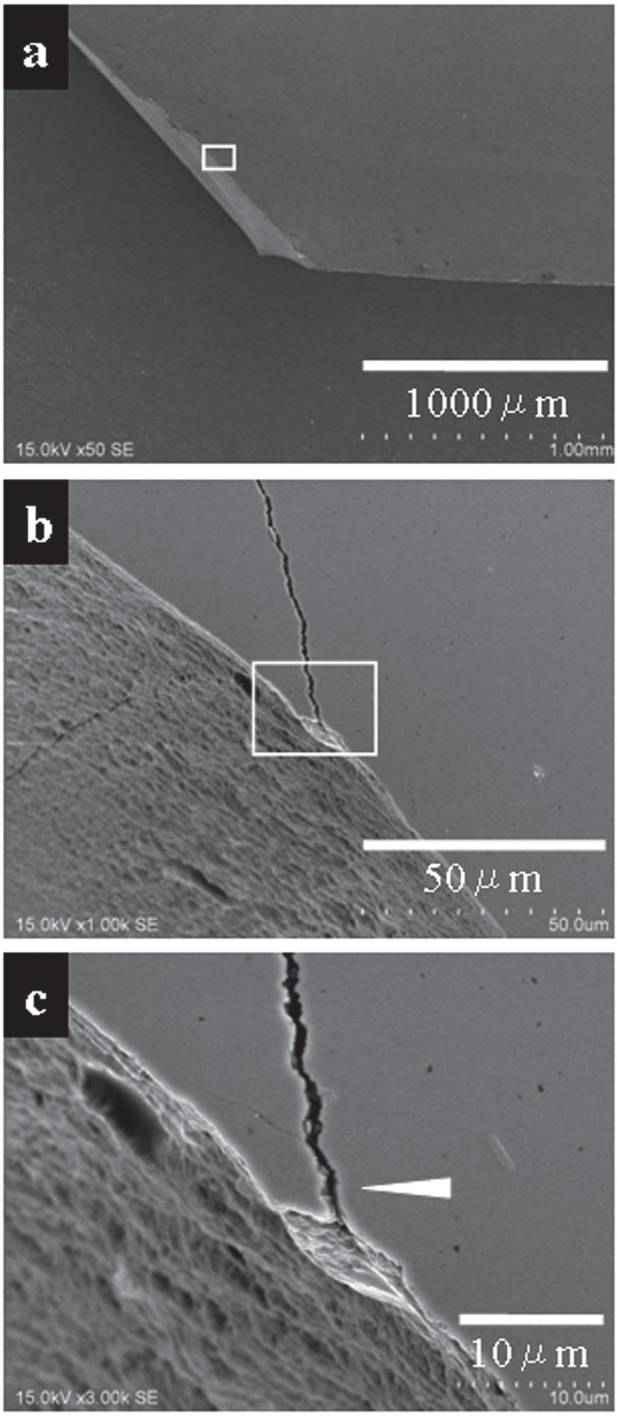

Fig. 7 SEM micrographs of fractured surface on MS specimen after cyclic fatigue test.
(a) ×50, (b) ×1,000, (c) ×3,000. Photographs (b) and (c) are higher magnification of areas shown in rectangle in (b) and (c), respectively, and white arrows show microcracks.

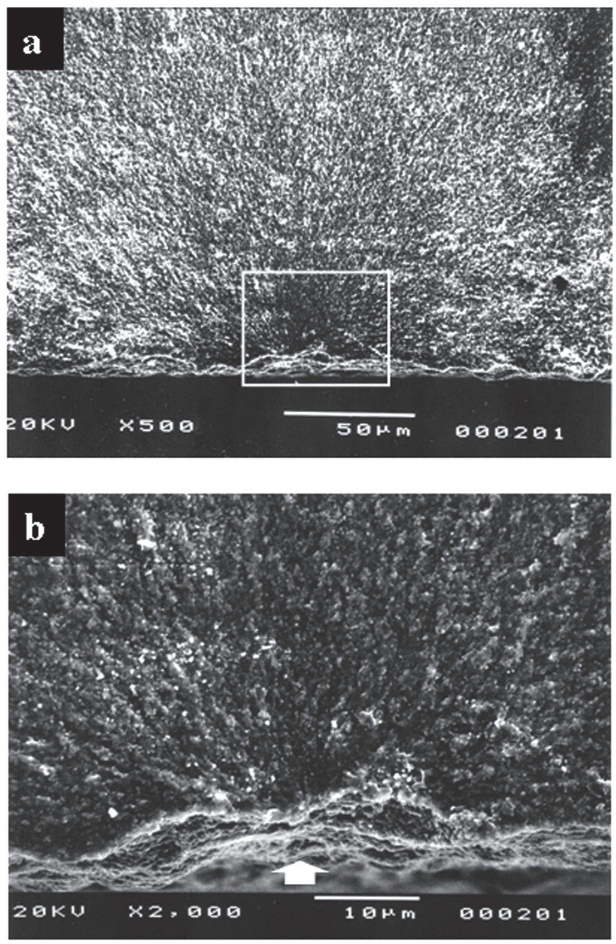

Fig. 8 SEM micrographs of fractured surface on SB150E specimen after cyclic fatigue test.
(a) ×500, (b) ×2000. Hackle lines radiated from fracture at defect (white arrow) located on tensile stress surface of this specimen.

Figure 8 shows a cross-sectional view of the fractured surface on a specimen after the cyclic fatigue test. Hackle lines were observed radiating from the fracture at the defect (white arrow) located on the tensile stress side surface of this specimen.

DISCUSSION

Sandblasting and acid-etching are commonly used to enhance the osteogenic potential of titanium implants. Similar treatment might be applied to zirconia if it is to be used in dental implants. Here, HF was used as the etching agent, as it is the most effective acid for obtaining fine structures in ceramics, including zirconia. If it is to be clinically applied to dental implants, HIP Y-TZP needs to be resistant to the cyclic loading that it will be subjected to in the oral environment. Therefore, the aim of this study was to clarify the effect of surface treatment on the fatigue properties of HIP Y-TZP.

The biaxial flexure test was used to evaluate static and fatigue strength, as recommended under ISO6872. The most common flexure test methods are the 3- and 4-point bending tests, which have a significant drawback because of difficulties in eliminating undesirable edge failures. As a result, the biaxial flexure test is frequently used to determine the fracture characteristics of ceramic materials. The biaxial flexure test has been adopted by the American Society for Testing and Materials for determining the strength of circular disks of brittle materials to be used as ceramic substrates, and is also the international standard for evaluating dental ceramics. The ISO specifications also recommend the biaxial flexure test (piston-on-three-ball) and 3-point bending test. A properly designed biaxial flexure test overcomes edge failure problems and thus assures a more accurate measurement of strength[28)].

The staircase method was employed to estimate fatigue strength in the present study. Many different fatigue testing procedures have been devised: the standard method using the S-N curve, constant stress level testing, the response or survival method (Probit method), step-test method, Prot method, staircase or up-and-down method, and the extreme value method[26)]. Among these, the staircase method automatically concentrates testing near the mean and requires fewer tests[29,30)], which is equally valid for determining the fatigue limit[26)].

In this study, the biaxial flexural strength of HIP Y-TZP MS was about two times greater than that previously reported for Y-TZP[23)]. Hot isostatic pressing was introduced to achieve very high density and enhance the reliability of ceramic components[16)]. Total number of defects and the largest defect size were reduced by HIP, resulting in an increase in the strength and Weibull modulus. This reduction in defects by HIP has also been reported to result in the origin of fracture shifting from the internal bulk to the surface[31)]. This means that HIP Y-TZP may be prone to low-temperature degradation initiated from defects on the surface in an aqueous solution, possibly resulting in a significant reduction in strength and toughness[13,32)]. Therefore, cyclic fatigue tests should be performed to confirm the applicability of HIP Y-TZP to implants.

In the present study, flexural strength showed a decrease in SB150 compared to in MS. Moreover, a further decrease in flexural strength was observed in SB150E under both the static loading and cyclic fatigue tests. In general, sandblasting is effective in inducing tetragonal-to-monoclinic transformation and, therefore, increasing the flexural strength of TZP. Indeed, while a monoclinic phase was recognized on the SB50, SB150 and SB150E surfaces, none was observed on the MS surfaces by X-ray diffractometry, suggesting that compressive stress occurred on the former. On the other hand, noticeable differences in surface morphology and Ra were observed between the MS specimens and the SB150 or SB150E specimens (Fig. 1). Whereas a completely smooth surface was seen in MS, nano structures were observed in SB150E on a large-waved configuration with comparatively deep defects (Fig. 1). Thus, sandblasting and acid-etching can introduce flaws or microcracks into HIP Y-TZP surfaces that might accelerate failure, suggesting that cracks rather than increase in the rate of monoclinic content by sandblasting[33)] are the deciding factor for strength in HIP Y-TZP. Taking these positive and negative effects of sandblasting and acid-etching into consideration, we believe that the introduction of flaws and microcracks by sandblasting and acid-etching may have been responsible for the decrease in flexural strength of HIP Y-TZP seen in this study.

Fracture strength in the cyclic fatigue test showed a remarkable decrease in comparison with that in the static test under all conditions in the present study. In brittle materials such as ceramics, cyclic loading leads to the propagation of small cracks, causing them to break at relatively low degrees of stress, and cyclic loading is effective in predicting the strength of ceramics in clinical use[34)]. In a static test, the presence of a compression layer on Y-TZP may contribute to an improvement fracture force. However, if a crack progresses from a surface defect by fatigue testing, it will influence low-temperature degradation, and a strong decrease in the strength can be expected. Inducing the hydroxyl (OH) group was also considered to decrease fatigue strength in the aqueous condition. It has been reported that acid-etching with HF introduces a hydroxyl group (OH) into Y-TZP surfaces[35)]. The increase in lattice spacing due to the penetration of OH ions created stress zones, inducing nucleation of monoclinic phase. The introduction of OH group may accelerate the low-temperature degradation. Accordingly, the penetration of OH ions into the HIP Y-TZP surfaces was considered to have contributed to the observed decrease in fatigue strength in the present study.

It was reported that the cyclic fatigue strength of Y-TZP at 5×10^5 cycles was 60–65% of the biaxial flexural strength in the static test[1,14,21)]. However, from the clinical point of view, in this study, the cyclic fatigue strength of HIP Y-TZP treated by sandblasting and acid-etching was much higher than 320 MPa, the required fatigue

strength of Y-TZP in surgical implants as specified in ISO 13356[20,22,31]. Dental implants may be different from surgical implants in terms of the degree of fatigue strength required. However, we believe that HIP Y-TZP is applicable to dental implants, as the fatigue strength of this material is more than double 320 MPa, the level required for Y-TZP in surgical implants. In addition, the cyclic fatigue strength of the SB150E specimens was more than twice that previous reported for Y-TZP[23]. Furthermore, HIP Y-TZP treated by sandblasting and acid-etching showed larger fatigue strength than Ce-TZP/Al_2O_3 nanocomposite (NANOZR)[23]. These results suggest that the enhanced fatigue strength of HIP Y-TZP make it a promising material for application to oral implant systems.

REFERENCES

1) Pittayachawan P, McDonald A, Young A, Knowles JC. Flexural strength, fatigue life, and stress-induced phase transformation study of Y-TZP dental ceramic. J Biomed Mater Res B Appl Biomater 2009; 88: 366-377.
2) Sevilla P, Sandino C, Arciniegas M, Martínez-Gomis J, Peraire M, Gil FJ. Evaluating mechanical properties and degradation of YTZP dental implants. Mater Sci Eng C 2010; 30: 14-19.
3) Oliva J, Oliva X, Oliva JD. One-year follow-up of first consecutive 100 zirconia dental implants in humans: a comparison of 2 different rough surfaces. Int J Oral Maxillofac Implants 2007; 22: 430-435.
4) Lalor PA, Revell PA, Gray AB, Wright S, Railton GT, Freeman MAR. Sensitivity to titanium. A cause of implant failure? J Bone Joint Surg 1991; 73-B: 25-28.
5) Olmedo DG, Paparella ML, Brandizzi D, Cabrini RL. Reactive lesions of peri-implant mucosa associated with titanium dental implants: a report of 2 cases. Int J Oral Maxillofac Surg 2010; 39: 503-507.
6) Gahlert M, Gudehus T, Eichhorn S, Steinhauser E, Kniha H, Erhardt W. Biomechanical and histomorphometric comparison between zirconia implants with varying surface textures and a titanium implant in the maxilla of miniature pigs. Clin Oral Implants Res 2007; 18: 662-668.
7) Akagawa Y, Ichikawa Y, Nikai H, Tsuru H. Interface histology of unloaded and early loaded partially stabilized zirconia endosseous implant in initial bone healing. J Prosthet Dent 1993; 69: 599-604.
8) Scarano A, Di Carlo F, Quaranta M, Piattelli A. Bone response to zirconia ceramic implants: an experimental study in rabbits. J Oral Implantol 2003; 29: 8-12.
9) Sennerby L, Dasmah A, Larsson B, Iverhed M. Bone tissue responses to surface-modified zirconia implants: A histomorphometric and removal torque study in the rabbit. Clin Implant Dent Relat Res 2005; 7 suppl 1: S13-S20.
10) Chevalier J, Gremillard L, Deville S. Low-temperature degradation of zirconia and implications for biomedical implants. Annu Rev Mater Res 2007; 37: 1-32.
11) Chevalier J, Cales B, Drouin JM. Low-temperature aging of Y-TZP ceramics. J Am Ceram Soc 1999; 82: 2150-2154.
12) Guo X. Property degradation of tetragonal zirconia induced by low-temperature defect reaction with water molecules. Chem Mater 2004; 16: 3988-3994.
13) Piconi C, Maccauro G. Zirconia as a ceramic biomaterial. Biomaterials 1999; 20: 1-25.
14) Studart AR, Filser F, Kocher P, Gauckler LJ. *In vitro* lifetime of dental ceramics under cyclic loading in water. Biomaterials 2007; 28: 2695-2705.
15) Masaki T. Mechanical properties of toughened ZrO_2-Y_2O_3 Ceramics. J Am Ceram Soc 1986; 69: 638-640.
16) Druschitz AP, Schroth JG. Hot isostatic pressing of a presintered yttria-stabilized zirconia ceramic. J Am Ceram Soc 1989; 72: 1591-1597.
17) Khraisat A, Stegaroiu R, Nomura S, Miyakawa O. Fatigue resistance of two implant/abutment joint designs. J Prosthet Dent 2002; 88: 604-610.
18) Norton MR. An *in vitro* evaluation of the strength of an internal conical interface compared to a butt joint interface in implants design. Clin Oral Implants Res 1997; 8: 290-298.
19) Möllersten L, Lockowandt P, Lindén LA. Comparison of strength and failure mode of seven implant systems: an *in vitro* test. J Prosthet Dent 1997; 78: 582-591.
20) Kosmac T, Oblak C, Jevnikar P, Funduk N, Marion L. Strength and reliability of surface treated Y-TZP dental ceramics. J Biomed Mater Res 2000; 53: 304-313.
21) Pittayachawan P, McDonald A, Petrie A, Knowles JC. The biaxial flexural strength and fatigue property of Lava Y-TZP dental ceramic. Dent Mater 2007; 23: 1018-1029.
22) Zhang Y, Pajares A, Lawn BR. Fatigue and damage tolerance of Y-TZP ceramics in layered biomechanical systems. J Biomed Mater Res B Appl Biomater 2004; 71: 166-171.
23) Takano T, Tasaka A, Yoshinari M, Sakurai K. Fatigue strength of Ce-TZP/Al_2O_3 nanocomposite with different surfaces. J Dent Res 2012; 91: 800-804.
24) Koch FP, Weng D, Kramer S, Biesterfeld S, Jahn-Eimermacher A, Wagner W. Osseointegration of one-piece zirconia implants compared with a titanium implant of identical design: a histomorphometric study in the dog. Clin Oral Implants Res 2010; 21: 350-356.
25) Teixeira EC, Piascik JR, Stoner BR, Thompson JY. Dynamic fatigue and strength characterization of three ceramic materials. J Mater Sci Mater Med 2007; 18: 1219-1224.
26) Collins JA. Failure of materials in mechanical design: Analysis, prediction, prevention. New York: John Wiley & Sons; 1981. p. 360-378.
27) Garvie RC, Nicholson PS. Phase analysis in zirconia systems. J Am Ceram Soc 1972; 55: 303-305.
28) Ban S, Anusavice KJ. Influence of test method on failure stress of brittle dental materials. J Dent Res 1990; 69: 1791-1799.
29) Little RE, Jebe EH. Fitting the P-S curve: Statistical design of fatigue experiments. New York-Toronto: A halsted press book, A division of John Wiley & Sons 1975. p. 168-197.
30) Yamamoto M, Takahashi H. Tensile fatigue strength of light cure composite resins for posterior teeth. Dent Mater J 1995; 14: 175-184.
31) Kim JY, Uchida N, Uematsu K. Effect of hiping defect and strength characteristics in y-tzp. J Ceram Soc Jpn 1992; 100: 311-314 (in Japanese).
32) Hirano M. Inhibition of Low temperature degradation of tetragonal zirconia ceramics a review. Br Ceram Trans J 1992; 91: 139-147.
33) Zinelis S, Thomas A, Syres K, Silikas N, Eliades G. Surface characterization of zirconia dental implants. Dent Mater 2010; 26: 295-305.
34) Benzaid R, Chevalier J, Saadaoui M, Fantozzi G, Nawa M, Diaz LA, Torrecilla R. Fracture toughness, strength and slow crack growth in a ceria stabilized zirconia-alumina nanocomposite for medical applications. Biomaterials 2008; 29: 3636-3641.
35) Shojai F, Mäntylä TA. Structuralstability of yttria doped zirconia membranes in acid and basic aqueous solutions. J Eur Ceram Soc 2001; 21: 37-44.